IEEE Access
Multidisciplinary | Rapid Review | Open Access Journal

Received April 25, 2021, accepted May 4, 2021, date of publication May 11, 2021, date of current version May 20, 2021.

Digital Object Identifier 10.1109/ACCESS.2021.3079175

Design, Analysis, and Control of a 3-DOF Novel Haptic Device Displaying Stiffness, Texture, Shape, and Shear

VIJAY KUMAR PEDIREDLA[1], (Graduate Student Member, IEEE), KARTHIK CHANDRASEKARAN[2], SRIKAR ANNAMRAJU[2], AND ASOKAN THONDIYATH[1], (Senior Member, IEEE)

[1]Indian Institute of Technology Madras, Chennai 600036, India
[2]Indian Institute of Information Technology, Design and Manufacturing, Chennai 600127, India

Corresponding author: Vijay Kumar Pediredla (pediredla.vijaykumar21@gmail.com)

ABSTRACT Haptic devices providing various sensations have multiple applications spanning over many fields such as surgical training, robot-assisted minimal invasive surgery (MIS), military, space, and underwater exploration. Most of the existing haptic interfaces lack the capability to effectively replicate the remote environment due to the intricacies involved in providing all necessary sensations simultaneously. In this paper, a novel haptic device with three degrees of freedom (DOF) is developed to render high-fidelity touch sensations like stiffness, texture, shape, and shear concurrently. The proposed haptic device consists of a spherical segment affixed with an array of texture surfaces based on the virtual/remote environment. The device can move in 3-DOF, namely, the pitch, roll, and vertical motion. The haptic interface provides kinesthetic cues like stiffness, shape, and environmental shear and tactile cues like texture by combining the movements of the three actuators along with the segmented housing. A systematic kinematic analysis of the proposed design is presented. The performance is enhanced by implementing the hybrid control methodology that switches between impedance and position control, thus making the interaction realistic and immersive. Experiments have been performed on the developed haptic device, and the results demonstrate its accuracy in reproducing various modalities of haptic feedback of the virtual/remote environment.

INDEX TERMS Haptic devices, kinesthetic and tactile feedback, impedance control, position control.

I. INTRODUCTION

Human-machine interfaces like smart mobiles, computers, virtual reality headsets, and teleoperated robotic systems use advanced technologies like computer graphics, virtual reality, and augmented reality to impact user interactions with virtual/remote environments. Most of the interfaces mentioned above cannot provide a realistic experience to the user because of the insufficiency of rendering various haptic modalities [1]. Unlike traditional interfaces, haptic interfaces can stimulate the human senses through multiple forces in the form of touch sensations to qualitatively perceive and manipulate the virtual/remote environment. The demand for haptic feedback in various systems has been increasing because of its feature of bidirectionality. Applications of haptic interfaces include medical, rehabilitation, military, industrial, entertainment, teleoperation systems, space, and underwater exploration [2]–[6]. In teleoperated systems, the haptic devices become the master robot, which is controlled by the user [7], [8]. Haptic devices in the context of feedback rendered are classified into two modalities, namely kinesthetic and tactile. Kinesthetic forces characterize the perception of position, shape, weight, and size by generating tension in the joints. Tactile forces describe the perception of texture, shear, stiffness, roughness, and vibration of the surface by distorting the receptors underneath the skin [4], [5]. Researchers have been developing various haptic devices to render remote/virtual environments through the haptic modalities, essentially either kinesthetic or tactile forces. Yet, rendering haptic feedback to most applications such as health care, teleoperated surgical systems, rehabilitation, military, and medical apprentice training is still a challenge because of the lack of intuitive interaction. They involve complex interaction forces, which demand the combination of kinesthetic

The associate editor coordinating the review of this manuscript and approving it for publication was Jenny Mahoney.

and tactile cues [9]. Also, tactile sensations [10], [11] typically play a vital role in various applications for presenting an experience of the environment tangibly through physical properties. For example, the surgeon can evaluate the tissue's condition through the forces experienced in the form of stiffness and surface textures. These forces help to identify the irregularities of the tissues like lumps, cancers, and so on [12]. Due to the lack of core physical attributes like tactile forces and kinesthetic forces, realism could disappear. Thus, there is a necessity in the haptics research community to develop a device that can simultaneously render both kinesthetic and tactile forces. Many devices have been developed in the past, combining kinesthetic and tactile feedback. However, the fundamental problem of rendering the perfect illusion of a virtual/remote environment remains unaddressed in practice because of several design and stability issues [2]–[6]. The kinesthetic and tactile sensations are coupled serially in the human hand, and this serial arrangement forbids the experience of natural feel when each stimulus is addressed independently [9]. The challenge here is to develop a haptic device that can provide a sense of kinesthetic feedback and natural interaction with the environment's textures. Therefore, in this work, an attempt is made to improve the user's natural feel by rendering some of the core attributes of the kinesthetic and tactile sensations such as stiffness, texture, shape, and shear.

With this motivation, we proposed a new 3-DOF haptic device in [13] and emphasized the importance of rendering a synergetic combination of kinesthetic and tactile feedback. The device provides haptic modalities like stiffness, texture, environmental shear, and shape to the finger accurately with a wide range of forces. In this paper, we further improve the work with the following contributions: i) kinesthetic device with tactile feedback enabled by various physical textures; ii) hybrid control algorithm that switches between position and impedance control is implemented for attaining compelling and distinct haptic forces to feel the environment naturally; iii) validation of various sensations through experiments.

The paper is organized as follows. In Section 2, a literature review of various haptic mechanisms and their feedback modalities are discussed briefly. The system design, along with kinematic and workspace analysis, has been elaborated in Section 3. In Section 4, the implementation of hybrid control for the proposed haptic device is illustrated. Experimental evaluation for justifying the claims, the discussions based on the performance of the device, and the future scope of the work are presented in Section 5. The conclusion is presented in Section 6.

II. BACKGROUND

Over the past few decades, different categories of mechanisms and devices have been introduced to provide haptic forces to the user to feel the manipulation and gripping forces. The primary actuation techniques used to reproduce the haptic forces are electric motors, pneumatic pressure cylinders, electrostatic, magnetic, piezoelectric, and smart material actuators [14]. Currently, exoskeleton and fingertip haptic devices are being developed to enhance the natural interactivity of various environments. Cyber grasp from Cyber glove systems and Wolverine [10] devices are used for moveable consumer applications, as its characteristics like low weight, low cost and power, and broad motion range address the desired features. However, reducing the complexity in the design and reproducing higher forces remains a challenge in exoskeleton haptic devices. Yoshida *et al.* [11], Gabardi *et al.* [15], and Schorr and Okamura [16] designed three DOF fingertip devices that render normal and lateral forces related to the remote/virtual environments. In [16], the friction discrimination of many virtual surfaces is also realized. Link touch [17] provides a directional haptic feel using a five-bar mechanism. These fingertip devices are rendering cutaneous feedback to increase the portability and wearability by minimizing the form factor. However, most of these devices were not very accurate because of open-loop force control. Additionally, viscoelastic parameters of finger pads that vary with the subjects affect the control accuracy [18].

Several studies [9], [13], [16], [19] have shown that adding tactile forces to the kinesthetic forces enhances the richness in sensations. In [9], two methods, namely serial and parallel kinematic coupling mechanisms, are proposed to render combined forces; however, the texture display is provided using an indirect way of vibro-actuation that limits accurate tactile perception. In [20], a combination of pneumatics and particle jamming is proposed that makes the user feel the tactile properties and shape. However, because of utilizing the particle jamming cells, the closed-loop rate is limited, and as a result, the user cannot instantaneously feel the variations of haptic sensations. More importantly, the textural information related to a variety of virtual/remote objects cannot be provided. Also, the height and force bandwidth of the rendered shape and stiffness profiles are limited and inadequate because of the jamming cells' complex behaviour. In the teleoperated systems and commercial haptic devices, providing kinesthetic feedback can destabilize the system and degrade the performance. Sensory substitution [19] has been introduced to address this issue, where tactile feedback is substituted for kinesthetic feedback to effectively represent the haptic interactions. However, generating tactile modalities, especially texture, becomes challenging compared to the other cues. This is due to the complexities of micro-machining, resolution, actuation techniques, and miniaturization [21], [22] involved in developing the tactile displays. Besides, concurrently rendering various tactile cues remains as a limitation in most of the existing devices. These limitations are addressed by introducing direct texture displays [23] that use natural passive textures (w.r.t environment) instead of actuators.

Some researchers have developed haptic devices for rendering the combination of modalities like shape and texture [15], shear contact and skin stretch [16], and texture and shear contact [23]. However, the lack of stiffness

modality makes the user's experience unrealistic. Although few haptic devices provide the stiffness modality both discretely and with the combination of other modalities like shape [10] and shear [11], they fail to create an impact of direct interaction with the environment because of lack of texture modality. In [24], an integrated kinesthetic and cutaneous display with the concept of modular design is developed to provide a wide range of stimuli. Researchers have been working to find the proper combination of the haptic modalities that can impact touch sensations. It is determined through experimental evaluations in [25], [26] that the combination of stiffness and tactile information could make the user's experience accurate and reliable. Therefore, stiffness and the texture modality of any object help identify, distinguish, and manipulate a virtual/remote environment based on the perceived properties. The user's perception of the environment is subdued by the natural dynamics like inertia and friction of the haptic device [27], [28].

Developing an appropriate control algorithm helps the user to feel the environment transparently. Many control methodologies like position, force, impedance, and admittance have been implemented to improve the haptic device's adaptability and robustness [27], [29]. The selection of controllers depends on the application being considered. Applications related to the medical domain, training, and rehabilitation involving compliant environments (to feel stiffness) use impedance control to modulate the dynamics [27]. For applications involving shape and shear rendering, position control would be sufficient. However, the proposed haptic device addresses the issue of rendering both kinesthetic and tactile feedback for which a hybrid control algorithm is essential to provide various haptic cues simultaneously. Many researchers have proposed control algorithms such as hybrid position/force control [30] and hybrid impedance control [31], [32] for making interactions with environments accurate and realistic. Nevertheless, these algorithms are difficult to implement practically and are very sensitive to design parameters (environment and haptic device). More importantly, the control algorithm should adapt itself to render a specific modality as desired by the user (through motion). Considering these issues, an attempt is made in this paper to develop an appropriate haptic device and a suitable control algorithm to provide stable interactions with improved transparency.

III. SYSTEM DESIGN DESCRIPTION

The goal of the proposed haptic device is to provide a combination of kinesthetic and tactile modalities in 3-DOF to the user.

The system design framework is shown in Figure 1. The integrated kinesthetic and tactile feedback has been achieved through the following design innovations:

1. A spherical segment equipped with various textures for surface property sensation is developed to provide kinesthetic and tactile feedback.

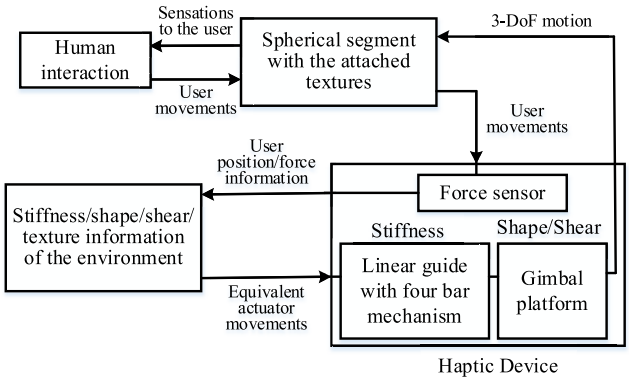

FIGURE 1. The system design framework.

2. A semi-compliant four-bar mechanism for rendering stiffness profile is proposed.
3. A gimbal platform to decouple between the roll and pitch DoF was utilized.
4. A force sensor was placed in a strategic position to measure the user's normal force, independent of the spherical segment orientation.
5. Three independent motors are employed in a hybrid control mode to generate the shape profile of the remote environment.

Since the key objective of this research work is to use actual textures instead of emulation by a vibrotactile display, pin array, and other actuation techniques. The proposed device has the following advantages:

1. Texture feedback is obtained passively, i.e., without the use of actuators
2. Higher fidelity of texture feedback
3. Enables the user to realize a lighter device due to the absence of actuators for generating texture feedback
4. Ease of implementation of texture feedback

As shown in Figure 2, the system consists of a spherical segment whose upper surface is equipped with various natural textures placed in an array based on the environment and are changeable for the chosen environment. The user experiences the textures with different surface properties (roughness, waviness, and lay) by placing the finger over the spherical platform. For example, in medical surgery scenarios, when the surgeon desires to interact with soft and hard tissues, bone, and blood vessels using the proposed haptic device, the segment is attached with various elastomers (tissues and vessels) and hard surfaces (bones) that represent the original textures.

The semi-compliant four-bar mechanism is built using the pseudo-rigid-body modelling technique to create the stiffness profile sensations. The use of a flexure mechanism (revolute joint and torsional spring) and the positioning of flexure in the assembly make the construction of the device simpler, free of backlash and friction. This mechanism also eliminates the need for lubrication, unlike the conventional slider-crank mechanism. There are two types of semi-compliant four-bar mechanisms, namely flexure-in-compression and

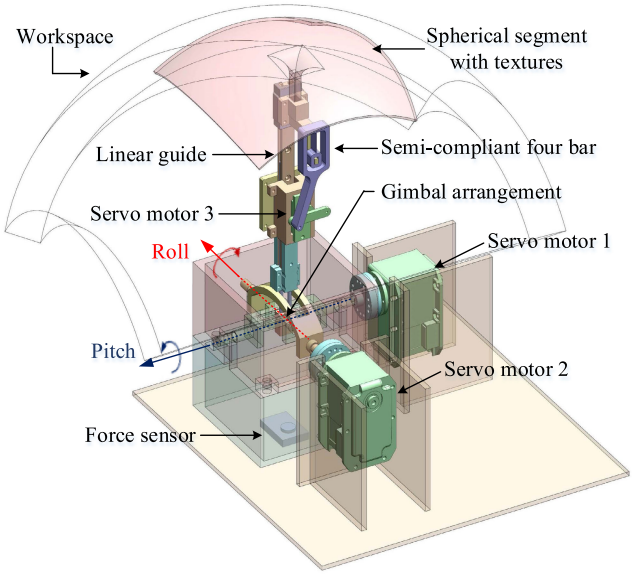

FIGURE 2. CAD model of the 3-DOF haptic device.

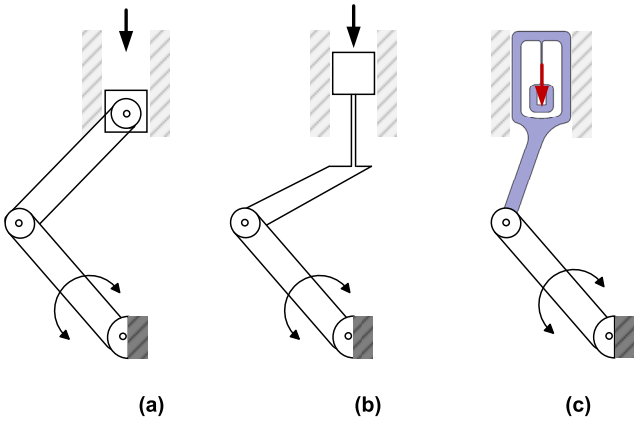

FIGURE 3. (a) Conventional slider-crank mechanism (b) Semi-compliant based four-bar mechanism with flexure in compression (c) Semi-compliant based four-bar mechanism with flexure in tension.

flexure-in-tension [33], available in the literature. In the former case, the force exerted by the user acts as a compression load. The disadvantages of using the flexure-in-compression are that the load-carrying capacity is low and, more importantly, the flexure buckles on load variations. However, the flexure-in-tension overcomes these limitations because of the way the flexure is positioned in the mechanism. The flexure-in-tension mechanism used in the proposed haptic device is placed in such a way that the force applied on the segment acts as a tensile load, as shown in Figure 3.

A linear guide connecting the spherical segment to the four-bar mechanism converts the rotary motion of servo motor 3 (Savox SH-0262MG model) to linear motion. Motor 3 is chosen with maximum speed and frequency as 167 rpm, and 250 Hz, respectively. Several stiffness profiles can be obtained by changing the impedance of motor 3 based on the force applied by the user while interacting with the segment. Force applied by the user is sensed by a piezoresistive-based force sensor (Honeywell-FSAGPDXX1.5LC5B5 model) placed underneath the haptic device. The placement of the force sensor at the bottom of the device ensures that the force vector is normal to the force sensor and independent of the position of the spherical segment. If the force sensor is placed at the interaction site, the vector may not be normal for most rendering scenarios.

Two servo motors (Dynamixel RX-64 model), namely motor 1 and motor 2, and the gimbal platform are utilized to move the segment in roll and pitch DOF. The gimbal platform guarantees to decouple between roll and pitch DOF and helps the user shift through textures on the segment rapidly, thus rendering the texture and shape modality of different objects of the environment through an assumed predefined finger trajectory. Besides, the haptic device provides environment shear sensations by varying the speed of two motors. Motor 1 and motor 2 are chosen with a maximum stall torque of 5.3 Nm, no-load speed of 64 rpm, and angular resolution of 0.29°. The shape profile of the remote/virtual environment is generated by combining the motion of all three motors. The entire workspace that the haptic device traverse in rendering the haptic modalities is indicated in Figure 2.

Although the proposed haptic device resembles the conventional haptic joystick mechanism, the following are some of the features that make the device unique:

1. The proposed device provides an area of contact representing a virtual environment rather than a single point of contact. Contrary to the haptic joystick that just provides relative mapping (as the usable workspace is small), absolute/relative mapping is attained.
2. There is no relative motion at the interface between the joystick and the user's finger. The proposed device can be used with either slip or no-slip contact. For instance, slip contact and non-slip contact can be used to explore and manipulate virtual models, respectively.
3. Existing haptic joysticks cannot provide shape information, while the proposed device can do so. Besides, texture and stiffness modalities can also be provided by the device. An array of textures that can provide textural stimuli are attached and swapped with additional/different textures to increase the number of available textures that can be felt through the device.

A. KINEMATIC ANALYSIS

The kinematic diagram of the proposed haptic device is illustrated in Figure 4. The active rotary joints are defined as A_1, A_2, and A_3 with their angular rotations given as θ, φ, and ψ, respectively. The joints A_1 and A_2 denotes roll and pitch angle, respectively, and the linear motion is provided by joint A_3 using a compliant-based four-bar mechanism. The passive joints are denoted as B_1, B_2, and B_3 with B_1 and B_2 being rotary joints and B_3 being prismatic joint. The reference frame is assumed as $S_0(O, x, y, z)$, and the link lengths are represented as l_1, l_2, l_3, m_1, and m_2 as shown in Figure 4. The position of the spherical segment that is in contact with the

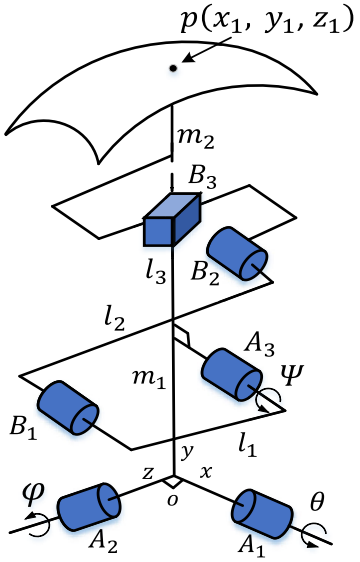

FIGURE 4. Kinematic model of the haptic device.

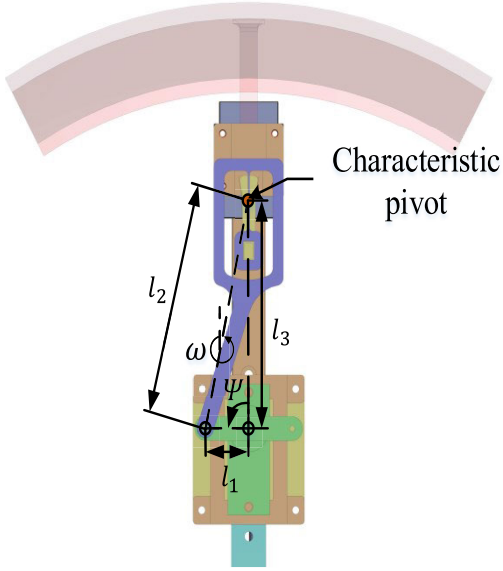

FIGURE 5. Semi-compliant four bar mechanism.

finger, $p(x_1, y_1, z_1)$, can be varied through the motion of the three active joint actuators w.r.t the frame S_0. The position of the angular segment can be expressed in three independent variables represented by $q = [\theta, r, \varphi]$, where r is the radial distance (linear sliding parameter), θ is the roll angle, and φ is the pitch angle, respectively.

The Cartesian coordinates of the end-effector (p) are given by:

$$x_1 = -r\cos(\theta)\sin(\varphi); \quad y_1 = r\cos(\theta)\cos(\varphi); \\ z_1 = r\sin(\theta) \tag{1}$$

The relation between r and the measurable independent variable ψ can be understood by analyzing the semi-compliant four-bar mechanism shown in Figure 5. In the semi-compliant four-bar mechanism, the active and passive joint angles, ψ and ω respectively, change the rotary motion into linear sliding motion.

The sliding parameter r, and dependent variable ω are given by:

$$r = l_1\cos(\psi) + l_2\cos(\omega) + m_1 + m_2; \\ \omega = \sin^{-1}\left(\frac{-l_1\sin(\psi)}{l_2}\right) \tag{2}$$

The inverse kinematics of the haptic device is given by

$$r = \sqrt{x_1^2 + y_1^2 + z_1^2}; \quad \theta = \arctan2\left(\frac{z_1}{\sqrt{x_1^2 + y_1^2}}\right); \\ \varphi = \arctan2\left(\frac{-x_1}{y_1}\right) \tag{3}$$

Thus, the spherical segment moves in 3-DOF by rendering linear motion radially, orientation about the x-axis and z-axis based on remote/virtual environment's physical and geometrical properties. Considering the link dimensions of the proposed haptic device, $l_1 = 12.5$ mm, $l_2 = 58$ mm, $l_3 = 56.64$ mm, the entire workspace limits are given by $0 \leq \Delta r \leq 25$ mm, $-55° \leq \theta \leq 55°$, $-55° \leq \varphi \leq 55°$, where Δr is the change in linear displacement. The workspace outline is shown in Figure 2.

B. DYNAMIC ANALYSIS

The dynamics of the haptic device are described using the Euler-Lagrangian method, and the general equations of motion is given by:

$$\frac{d}{dt}\frac{\partial L}{\partial \dot{q}} - \frac{\partial L}{\partial q} = \tau; \quad L = T - U \tag{4}$$

where L, T, U are defined as the Lagrangian function, kinetic energy and potential energy respectively, q is the generalized coordinates represented as $[\theta, r, \varphi]$. The kinetic (T) and potential (U) energy of the haptic device are given by

$$T = \frac{1}{2}ml^2(\dot{\theta}^2 + \dot{\varphi}^2\cos^2(\theta) + \dot{r}^2); \\ U = mgl\cos(\theta)\cos(\varphi) \tag{5}$$

The Lagrangian dynamics of the haptic device is given by

$$m(q)\ddot{q} + C(q, \dot{q})\dot{q} + g(q) = \tau \tag{6}$$

where m, C, g, l are defined as positive inertia, centrifugal and Coriolis matrix, gravity force vector, and distance from the origin to the center of mass, respectively. $\tau \in R^{3x1}$ are the control input torques. The mass (m) is calculated from the kinetic energy (T) as in (5), using lumped mass approximations. The equivalent parameter of the distance from the origin to the center of mass (l) is taken from the CAD model. The Coriolis matrix is calculated using (4)-(6) and the mass matrix. The gravitational vector is calculated from the potential energy (U), (5) using the mass matrix.

IV. CONTROL IMPLEMENTATION

In this section, a control architecture for the 3-DOF haptic device is proposed and implemented to improve the stability and accuracy of rendering the haptic cues. As shown in Figure 6, a hybrid controller is developed by combining the position and impedance control to provide high-fidelity haptic sensations to the user. The controller uses a PD (proportional-Derivative) position controller for shape and environmental shear and an impedance controller for stiffness control. While position control is continually applied for motor 1 and 2, and motor 3 switches between position control and impedance control based on the rendered haptic modality. The hybrid (switching) control is chosen despite the instabilities between switching because, in practice, the stiffness and shape sensations cannot be felt simultaneously by any user. Impedance control methodology is the most effective method to realize physical properties like stiffness, as it controls the contact dynamics [29]. To make the user's experience realistic and reliable, impedance control is considered, which modulates the relation between the motion and force of the device.

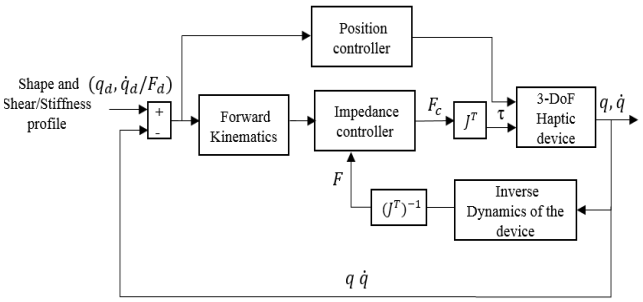

FIGURE 6. Block diagram of hybrid control methodology.

Considering the kinematics and dynamics of the haptic device derived earlier, the desired angular variables are computed according to the shape and shear of the environment. Based on the finger's defined trajectory, the angular variables are calculated from the inverse kinematics of the haptic device. The calculated angular variables are given as an input for the three actuators, and the coordinated movement of the spherical platform is achieved to precisely move the point 'p'. The error is determined between the desired and sensed rotary angles and angular velocities, and these error signals are sent to the PD (proportional and derivative) controller. The closed-loop PD position controller for the three actuators of the haptic interface is given by

$$\tau = K_1 (q_d - q) + K_2(\dot{q}_d - \dot{q}) \tag{7}$$

where $q, q_d \in R^{3\times1}$ are measured and desired independent variable vectors, respectively, K_1 and K_2 are the positive definite gain feedback matrices.

A closed-loop impedance controller is primarily implemented for motor 3 of the proposed haptic device in which the user's motion commands serve as input and generates force feedback. Impedance control with force feedback (through a force sensor) subdues the unwanted dynamics and frictional effects, including the dynamics of the haptic device, and consequently, enhances the transparency in rendering various remote/virtual environments. However, the backlash could be a potential problem for closed-loop impedance control and is addressed while designing the haptic device by providing backlash-free mechanisms (a four-bar mechanism). Therefore, the goal of the implemented control is to negate all the unwanted dynamics and provide the closed-loop impedance as the desired stiffness of the virtual object. However, this is practically not viable, and hence the control algorithm should minimize the effects of unwanted dynamics while rendering the desired stiffness. The developed impedance controller for stiffness perception (spring model: $F_d = k_d(\Delta r_d - \Delta r)$) is given by

$$\tau = J^T(F_d + K_f (F_d - F)) \tag{8}$$

$$\Delta r = J(Z_u + Z_h)^{-1}(\tau - J^T F) \tag{9}$$

where J, F_d, F, K_f, k_d, Z_h, Z_u, Δr_d and Δr are Jacobian matrix, desired force, measured force, force gain, desired stiffness constant, haptic device impedance, user's impedance, desired and actual indentation depth of the segment, respectively.

From (6), (7), and assuming $\Delta r_d = 0$, the closed-loop haptic impedance is given by

$$Z_{CL} = k_d + (1 + K_f)^{-1}(Z_u + Z_h) \tag{10}$$

Thus, the controller utilizes the force sensor information to eliminate unwanted dynamics, i.e., haptic device natural dynamics, modelling errors, and frictional effects. In general, to completely nullify the undesirable dynamics, the gain K_f should be very high. However, since the operating frequency of the device is sufficiently low, even a relatively low K_f is sufficient, thus, improving transparency and maintaining the system's stability.

The gain tuning of the proposed hybrid controller utilizes the position accuracy (position control) and impedance characteristics (impedance control) of the rendered environment. For an arbitrary shape profile, position control gains are chosen using a trial-and-error methodology. For the environment considered (pure virtual spring), the gain for impedance control is calculated using the characteristics such as k_d(desired stiffness) and ω_d (desired bandwidth), and is given by

$$\omega_d = \sqrt{k_d/Z_h + Z_u} \tag{11}$$

Thus, the force gain is calculated using the equation,

$$K_f = \alpha\omega_d \tag{12}$$

where α is a scaling factor.

Larger the ω_d, the more is the frequency bandwidth in which the device shows good impedance tracking. The force for the impedance controller is calculated from (12); however, the scaling factor is varied from 0.8 to 1.5 for increasing desired stiffness.

In summary, when the user moves his finger without changing the vertical displacement of the haptic interface, position control is applied. Consequently, the shape, shear, and texture of the virtual environment are realized. Additionally, when the user probes the haptic interface radially, impedance control is applied, and therefore, a force is generated, providing stiffness of the virtual environment. The proposed hybrid control switches spontaneously between position and impedance control based on the user's motion to experience the haptic sensations. Experiments have been carried out to evaluate the effectiveness of the haptic device and the hybrid control strategy.

V. EXPERIMENTAL EVALUATION

Considering the virtual stiffness, texture, shape, and shear profiles of the virtual/remote object, experiments were performed on the haptic device to analyze and validate the performance of each modality distinctly. The prototype of the proposed haptic device is shown in Figure 7. In the first experiment, the shape and environmental shear rendering abilities with a position control strategy are evaluated with gains K_1 and K_2 as 1.5 and 2.8 respectively. In the second experiment, the haptic device's stiffness rendering capability with an impedance control strategy is assessed with the force gain (K_f) range between 2 to 10. Texture modality is rendered to the user in both the experiments along with the specified sensations. Also, the results of both experiments are analyzed to validate the efficacy of the proposed haptic device.

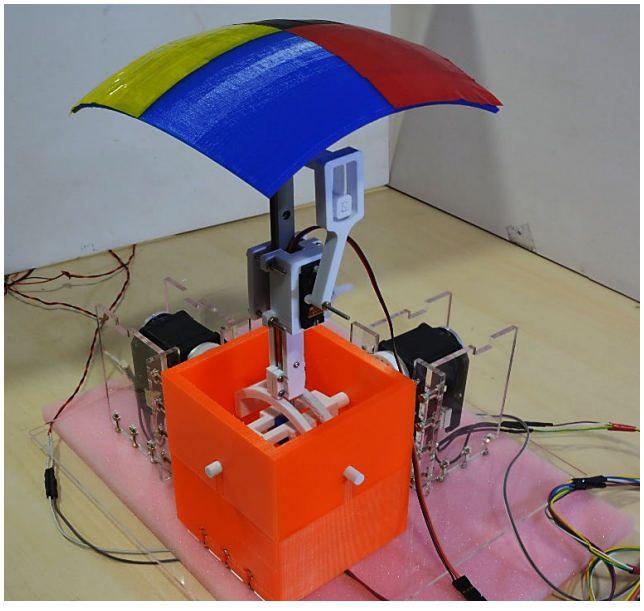

FIGURE 7. Experimental setup of the proposed haptic device.

A. RENDERING SHAPE AND ENVIRONMENTAL SHEAR USING POSITION CONTROL METHOD

The user can interact with the haptic device's spherical platform to feel the shape and environmental shear profile (reference trajectory) of the remote/virtual environment. In general, an ideal shape display should have a high spatial resolution of around 2 to 3 mm and support contact forces of a minimum 50 gf produced by the user's finger all through the shape exploration (necessary conditions). The refresh rate should be a minimum of 1 kHz for maintaining the realistic haptic feedback (sufficient condition) [34]. However, these conditions vary based on the haptic devices and applications. Two experiments are performed to assess the performance and accuracy of the position controller for rendering shape and environmental shear.

A reference shape trajectory (sum of sinusoidal) of a virtual environment is provided. By tracking the user's motion, the shape is accordingly represented by the coordinated movements of the three actuators. Figure 8 (a) shows the reference and rendered shape trajectories in xy and yz planes, respectively. Along with the static and dynamic (adapting to the user's finger movements) shape variations, the texture of the virtual environment is also provided. The results demonstrate the efficacy of the haptic device in rendering shape. The Root Means Square (RMS) error and standard deviation while rendering the shape was 0.36 mm and 0.2 mm, respectively. The error profile of the position in x-y and y-z planes are shown in Figure 8 (b).

Additionally, another experiment is conducted to evaluate the repeatability of the device in providing an accurate shape profile, considering the proposed position control algorithm. Ten random shape profiles are generated with the limits being, $0 \leq \Delta r \leq 12$ mm, $-30^\circ \leq \theta \leq 30^\circ$, $-30^\circ \leq \varphi \leq 30^\circ$. The mean error and standard deviation between the reference shape trajectory and measured shape trajectory for these iterations were obtained as 0.41 mm and 0.22 mm, respectively. Figure 8 (c) also shows the position tracking in the time domain, illustrating the haptic device's response time. The spatial resolution of the proposed device's shape display is 2.9 mm and supports contact forces of 70 gf by the user. The lag between reference and rendered trajectories is observed to be around 110 ms. When the user attempts to swap between various textures attached to the spherical segment, the segment moves accordingly (the spherical segment provides relative movements to enhance the workspace of each texture) to render texture and shape information.

Similarly, a reference shear trajectory is assumed based on the fractional derivative model [35] given by

$$\tau_s = \mu_\alpha \frac{d^\alpha u}{dy^\alpha}, \quad 0 < \alpha < 2 \tag{13}$$

where τ_s, μ, du/dy and α are the shear stress, dynamic viscosity, velocity gradient, and order of fractional derivative, respectively.

The values of the stresses are exerted on a surface oriented in the positive x, y, and z directions. The environmental shear stress is measured from the force sensor, and the contact area of the index finger that interacts with the haptic device is measured to be 3 cm^2. When the user applies the force, the sense of change in position is rendered via position control, ensuring accuracy. Reference shear profile for four diverse objects

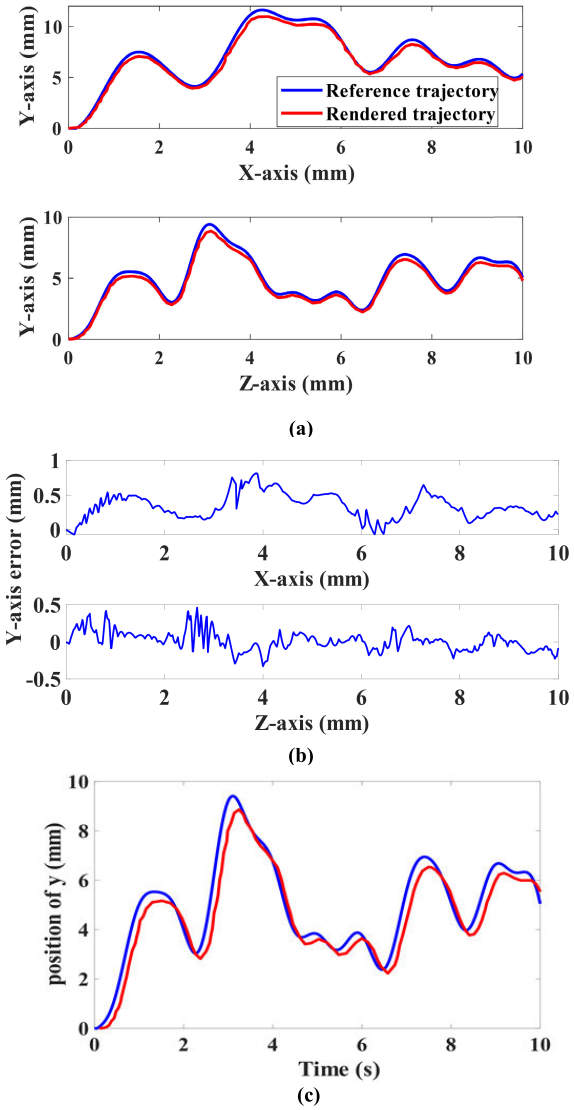

FIGURE 8. (a) Shape profiles in x-y and y-z planes (b) Position error in x-y and y-z planes (c) Position tracking in the time domain.

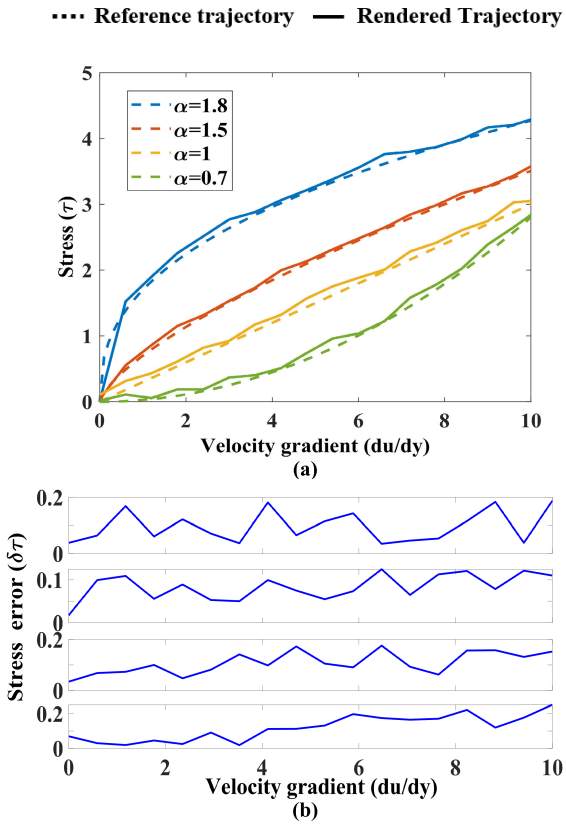

FIGURE 9. (a) Shear stress profiles for four different objects with different fractional derivative order (b) Error profile of Shear stress.

is assumed with varying textures and fractional derivative orders approximately corresponding to biological fluid (especially for $\alpha > 1$) [36]. The position control strategy controls the position and velocity of the three actuators to provide reference shear stress based on the predefined finger trajectory. The mean error and standard deviation of shear stress are 0.26 and 0.14 N/mm^2, respectively. Figure 9 (a) and (b) display the reference and rendered environmental shear stress profiles and the error profile of the stress, respectively. The results demonstrate the effectiveness of providing the shear sensation.

B. RENDERING STIFFNESS USING IMPEDANCE CONTROL METHOD

Let us assume a virtual/remote environment with four diverse surfaces having different mechanical properties (texture and stiffness). An experiment is conducted to assess the performance of the haptic device in rendering stiffness of different linear springs. When the user varies the position (probing radially) of the haptic device, the variable displacement becomes an input for the virtual/remote environment, and the corresponding desired force is generated. A force sensor underneath the haptic device measures force experienced by the user and this data is sent to the controller, thus changing the control torque accordingly. The implemented impedance controller modifies the user's perceived impedance in accordance with the stiffness characteristics (desired impedance) of the remote/virtual environment. Considering four different objects with stiffness constants, $k1 = 0.75$ N/mm, $k2 = 1$ N/mm, $k3 = 1.5$ N/mm, and $k4 = 2$ N/mm. The stiffness profiles and their corresponding errors rendered by the haptic device are shown in Figure 10 (a) and (b), respectively.

The results demonstrate the accuracy of the haptic device with an impedance controller in providing stiffness along with texture. The mean error and standard deviation of the stiffness are found to be 0.17 and 0.11 N/mm. The maximum force and indentation depth rendered by the haptic device is up to 8 N and 25 mm, respectively.

C. DISCUSSIONS AND FUTURE WORKS

Few experiments have been performed to validate the accuracy of the proposed haptic device in displaying high-fidelity haptic feedback. Error analysis of the experiments generating

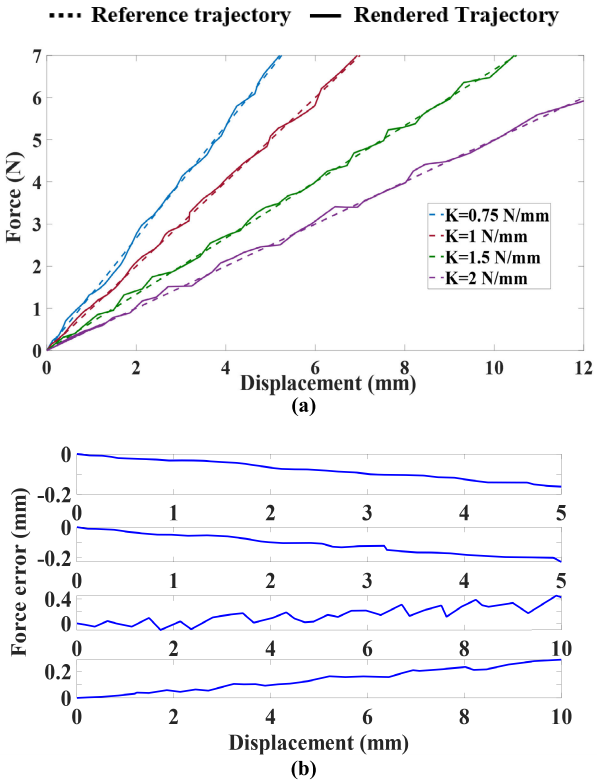

FIGURE 10. (a) Stiffness profile for four different objects (b) Error profile of stiffness sensation.

haptic modalities like shape, environmental shear, and stiffness has been indicated. The average height and stiffness errors are around 0.5 mm and 0.2 mm, respectively, with modulation speed between the textures and spatial resolution of around 38.5 mm/s and 0.4 mm. This demonstrates the rendering of accurate profiles such as shape and stiffness by the haptic device compared to the traditional haptic devices with errors around 2 mm and 0.8 mm, respectively, with a spatial resolution around 2.8 mm [10], [20]. Also, the resolution of the proposed haptic device is within the resolution limits of Kinect's depth sensor and ratchet system. The maximum height and stiffness range of the proposed device are around 12 mm and 7 N/mm, respectively. Concerning textural rendering, since the natural textures are directly attached to the segment, the spatial perception is a continuum.

The hybrid control algorithm, as mentioned earlier, contributes to making the haptic device transparently feel the environment by improving adaptability and stability. The impedance controller with force feedback enhanced the accuracy of matching desired impedance. However, as the desired stiffness decreases, the dynamics of the haptic device becomes prominent. Therefore, to overcome this limitation, the inertia of the device should be reduced. Also, because of the nature of switching between controls, instabilities are possible, especially while shifting from position control to impedance control because of the varying equilibrium points while shape rendering. These cases will be studied in detail and will be reported in future works.

The limitations associated with the proposed design of the haptic device are as follows:

i) The user's experience of the textural information is limited because the workspace related to each texture is constrained on the spherical segment. Also, the textures have to be replaced based on various environments.
ii) The information related to edges of the remote/virtual environment cannot be provided because the spherical segment (curved arc) interface doesn't have any edges.
iii) Because of the bulkiness of the device, wearability becomes a challenge.
iv) Nonlinear stiffness profiles cannot be rendered because of the actuator constraints.

The knowledge gained from the haptic sensations rendered by the device immerses the user into the virtual/remote scenarios. It can be helpful in many applications, particularly in the medical field, training apprentices (simulators), and rehabilitation applications [37]. In telerobotic and minimally invasive surgeries, haptic feedback, especially in the form of stiffness perception along with texture sensations, makes the surgeon feel the tissue properties properly [38]. Knowing tissue stiffness helps to diagnose minor infections up to tumors, lumbar puncture inspection, and so on [39]. Here, texture modality plays an essential role in identifying the initial stage of any infection, where the textural behavior of tissue changes while stiffness may not be affected. Similarly, novice surgeons are trained in identifying the disease appropriately by feeling the tissue's stiffness and textural properties. Additionally, some procedures, such as needle insertion, tumor detection, and so on, can be implemented virtually for training surgeons. In applications involving exploration, the information regarding the texture is unknown; hence, the stiffness and shape of various objects can only be rendered to give the feel of the object properties. This device can also be broadly used in rehabilitation [40] and gaming applications by creating virtual environments with various textures, shapes, and stiffness properties to give a realistic feel to the user.

Future works include modifying spherical segment carrying textures with a belt mechanism supporting few textures that can render longer length, thus enhancing the workspace. The same belt mechanism can be used to generate a variety of textures with smaller lengths. Also, the spherical segment can be replaced with an interface with edges (ex: hexagonal segment) similar to the remote environment that can address the limitation of generating sharp edges and corners. With the concept of rendering multimodal sensations and utilizing the mechanism proposed in this article, we are analyzing the possibility of developing a haptic grasper to widen the applications.

VI. CONCLUSION

In this paper, we presented the design, control, and experimental evaluation of a novel 3-DOF haptic device capable of rendering various haptic modalities. The proposed haptic device is unique in providing a combination of stiffness and

texture, shape, and environmental shear, thus augmenting the haptic feedback to sense and manipulate the virtual/remote environment. Texture and environmental shear are represented through a spherical platform attached with an array of textures and is traversed in 2-DOF by changing the motion parameters of pitch and roll. Stiffness sensation is represented through another DOF perpendicular to the movement of the spherical segment, and the shape is displayed by the coordinated action of the three actuators. A hybrid control algorithm is implemented, comprising of position and impedance control to enhance the rendering capability of sensations through the haptic device and are separately analyzed to evaluate the performance objectively. The experimental studies indicate the efficacy of the developed haptic device.

REFERENCES

[1] A. Hamam, M. Eid, and A. El Saddik, "Effect of kinesthetic and tactile haptic feedback on the quality of experience of edutainment applications," *Multimedia Tools Appl.*, vol. 67, no. 2, pp. 455–472, Nov. 2013.
[2] S. L. Springer and N. J. Ferrier, "Design and control of a force-reflecting haptic interface for teleoperational grasping," *J. Mech. Des.*, vol. 124, no. 2, pp. 277–283, Jun. 2002.
[3] R. Tadayon, "Haptics for accessibility in hardware for rehabilitation," in *Haptic Interfaces for Accessibility, Health, and Enhanced Quality of Life*. Cham, Switzerland: Springer, 2020, pp. 243–263.
[4] B. Stephens-Fripp, G. Alici, and R. Mutlu, "A review of non-invasive sensory feedback methods for transradial prosthetic hands," *IEEE Access*, vol. 6, pp. 6878–6899, 2018.
[5] A. Villegas, P. Perez, R. Kachach, F. Pereira, and E. Gonzalez-Sosa, "Real haptics: Using physical manipulation to control virtual worlds," in *Proc. IEEE Conf. Virtual Reality 3D User Interfaces Abstr. Workshops (VRW)*, Mar. 2020, p. 856.
[6] N. Enayati, E. De Momi, and G. Ferrigno, "Haptics in robot-assisted surgery: Challenges and benefits," *IEEE Rev. Biomed. Eng.*, vol. 9, pp. 49–65, 2016.
[7] Z. Chen, F. Huang, W. Sun, J. Gu, and B. Yao, "RBF-neural-network-based adaptive robust control for nonlinear bilateral teleoperation manipulators with uncertainty and time delay," *IEEE/ASME Trans. Mechatronics*, vol. 25, no. 2, pp. 906–918, Apr. 2020.
[8] C. Hua, Y. Yang, and P. X. Liu, "Output-feedback adaptive control of networked teleoperation system with time-varying delay and bounded inputs," *IEEE/ASME Trans. Mechatronics*, vol. 20, no. 5, pp. 2009–2020, Oct. 2015.
[9] P. Kammermeier, A. Kron, J. Hoogen, and G. Schmidt, "Display of holistic haptic sensations by combined tactile and kinesthetic feedback," *Presence, Teleoperators Virtual Environ.*, vol. 13, no. 1, pp. 1–15, Feb. 2004.
[10] I. Choi, E. W. Hawkes, D. L. Christensen, C. J. Ploch, and S. Follmer, "Wolverine: A wearable haptic interface for grasping in virtual reality," in *Proc. IEEE/RSJ Int. Conf. Intell. Robots Syst. (IROS)*, Oct. 2016, pp. 986–993.
[11] K. T. Yoshida, C. M. Nunez, S. R. Williams, A. M. Okamura, and M. Luo, "3-DoF wearable, pneumatic haptic device to deliver normal, shear, vibration, and torsion feedback," in *Proc. IEEE World Haptics Conf. (WHC)*, Jul. 2019, pp. 97–102.
[12] W. K. I. Baumann and P. K. Plinkert, "Vibrotactile characteristics of different tissues in endoscopic otolaryngologic surgery-*in vivo* and *ex vivo* measurements," *Minimally Invasive Therapy Allied Technol.*, vol. 10, no. 6, pp. 323–327, Jan. 2001.
[13] V. K. Pediredla, K. Chandrasekaran, S. Annamraju, and A. Thondiyath, "A novel three degrees of freedom haptic device for rendering texture, stiffness, shape, and shear," in *Proc. IFToMM Int. Symp. Robot. Mechatronics*. Cham, Switzerland: Springer, 2019, pp. 412–422.
[14] S. P. Buerger and N. Hogan, "Novel actuation methods for high force haptics," in *Advances in Haptics*, M. H. Zadeh, Ed. Rijeka, Croatia: InTech, 2010.
[15] M. Gabardi, M. Solazzi, D. Leonardis, and A. Frisoli, "A new wearable fingertip haptic interface for the rendering of virtual shapes and surface features," in *Proc. IEEE Haptics Symp. (HAPTICS)*, Apr. 2016, pp. 140–146.
[16] S. B. Schorr and A. M. Okamura, "Three-dimensional skin deformation as force substitution: Wearable device design and performance during haptic exploration of virtual environments," *IEEE Trans. Haptics*, vol. 10, no. 3, pp. 418–430, Jul. 2017.
[17] D. Tsetserukou, S. Hosokawa, and K. Terashima, "LinkTouch: A wearable haptic device with five-bar linkage mechanism for presentation of two-DOF force feedback at the fingerpad," in *Proc. IEEE Haptics Symp. (HAPTICS)*, Feb. 2014, pp. 307–312.
[18] D. Prattichizzo, F. Chinello, C. Pacchierotti, and M. Malvezzi, "Towards wearability in fingertip haptics: A 3-DoF wearable device for cutaneous force feedback," *IEEE Trans. Haptics*, vol. 6, no. 4, pp. 506–516, Oct. 2013.
[19] Z. F. Quek, S. B. Schorr, I. Nisky, W. R. Provancher, and A. M. Okamura, "Sensory substitution and augmentation using 3-degree-of-freedom skin deformation feedback," *IEEE Trans. Haptics*, vol. 8, no. 2, pp. 209–221, Apr. 2015.
[20] A. A. Stanley and A. M. Okamura, "Controllable surface haptics via particle jamming and pneumatics," *IEEE Trans. Haptics*, vol. 8, no. 1, pp. 20–30, Jan. 2015.
[21] H. Culbertson, S. B. Schorr, and A. M. Okamura, "Haptics: The present and future of artificial touch sensation," *Annu. Rev. Control, Robot., Auton. Syst.*, vol. 1, no. 1, pp. 385–409, May 2018.
[22] C.-H. King, M. Franco, M. O. Culjat, A. T. Higa, J. W. Bisley, E. Dutson, and W. S. Grundfest, "Fabrication and characterization of a balloon actuator array for haptic feedback in robotic surgery," *J. Med. Devices*, vol. 2, no. 4, Dec. 2008, Art. no. 041006.
[23] E. Whitmire, H. Benko, C. Holz, E. Ofek, and M. Sinclair, "Haptic revolver: Touch, shear, texture, and shape rendering on a reconfigurable virtual reality controller," in *Proc. CHI Conf. Hum. Factors Comput. Syst.*, 2018, pp. 1–12.
[24] M. Fritschi, M. O. Ernst, and M. Buss, "Integration of kinesthetic and tactile display: A modular design concept," in *Proc. EuroHaptics Int. Conf. (EH)*, Jul. 2006, pp. 607–612.
[25] S. L. Lederman and R. L. Klatzky, "Relative availability of surface and object properties during early haptic processing," *J. Exp. Psychol., Hum. Perception Perform.*, vol. 23, no. 6, pp. 1680–1707, 1997.
[26] M. A. Srinivasan and R. H. LaMotte, "Tactual discrimination of softness," *J. Neurophysiol.*, vol. 73, no. 1, pp. 88–101, Jan. 1995.
[27] H. Saafi, M. A. Laribi, and S. Zeghloul, "Haptic control implementation of a 3-RRR spherical parallel manipulator for medical uses," in *Experimental Robotics*. Cham, Switzerland: Springer, 2016, pp. 61–72.
[28] C. R. Carignan and K. R. Cleary, "Closed-loop force control for haptic simulation of virtual environments," *Electron. J. Haptics Res.*, vol. 1, no. 2, pp. 1–14, 2000.
[29] M. K. O'Malley, A. Gupta, M. Gen, and Y. Li, "Shared control in haptic systems for performance enhancement and training," *J. Dyn. Syst., Meas., Control*, vol. 128, no. 1, pp. 75–85, Mar. 2006.
[30] B.-P. Huynh, C.-W. Wu, and Y.-L. Kuo, "Force/position hybrid control for a Hexa robot using gradient descent iterative learning control algorithm," *IEEE Access*, vol. 7, pp. 72329–72342, 2019.
[31] M. Hosseinzadeh, P. Aghabalaie, H. A. Talebi, and M. Shafie, "Adaptive hybrid impedance control of robotic manipulators," in *Proc. 36th Annu. Conf. IEEE Ind. Electron. Soc. (IECON)*, Nov. 2010, pp. 1442–1446.
[32] K. Mouri, K. Terashima, P. Minyong, H. Kitagawa, and T. Miyoshi, "Identification and hybrid impedance control of human skin muscle by multi-fingered robot hand," in *Proc. IEEE/RSJ Int. Conf. Intell. Robots Syst.*, Oct. 2007, pp. 2895–2900.
[33] J. Dearden, C. Grames, B. D. Jensen, S. P. Magleby, and L. L. Howell, "Inverted L-arm gripper compliant mechanism," *J. Med. Devices*, vol. 11, no. 3, Sep. 2017, Art. no. 034502.
[34] K. Zhang, E. J. Gonzalez, J. Guo, and S. Follmer, "Design and analysis of high-resolution electrostatic adhesive brakes towards static refreshable 2.5 D tactile shape display," *IEEE Trans. Haptics*, vol. 12, no. 4, pp. 470–482, Oct./Dec. 2019.
[35] H. Sun, Y. Zhang, S. Wei, J. Zhu, and W. Chen, "A space fractional constitutive equation model for non-Newtonian fluid flow," *Commun. Nonlinear Sci. Numer. Simul.*, vol. 62, pp. 409–417, Sep. 2018.
[36] X. J. Li and Y. Zhou, Eds., *Microfluidic Devices for Biomedical Applications*. Amsterdam, The Netherlands: Elsevier, 2013.
[37] H. Lee, A. Eizad, S. Pyo, M. R. Afzal, M.-K. Oh, Y.-J. Jang, and J. Yoon, "Development of a robotic companion to provide haptic force interaction for overground gait rehabilitation," *IEEE Access*, vol. 8, pp. 34888–34899, 2020.

[38] R. Riener and M. Harders, "VR for medical training," in *Virtual Reality in Medicine*. London, U.K.: Springer, 2012, pp. 181–210.
[39] M. T. Thai, T. T. Hoang, P. T. Phan, N. H. Lovell, and T. N. Do, "Soft microtubule muscle-driven 3-axis skin-stretch haptic devices," *IEEE Access*, vol. 8, pp. 157878–157891, 2020.
[40] L. Jiang, M. R. Cutkosky, J. Ruutiainen, and R. Raisamo, "Using haptic feedback to improve grasp force control in multiple sclerosis patients," *IEEE Trans. Robot.*, vol. 25, no. 3, pp. 593–601, Jun. 2009.

VIJAY KUMAR PEDIREDLA (Graduate Student Member, IEEE) received the B.Tech. degree in instrumentation and control engineering from the National Institute of Technology, Tiruchirappalli, India, in 2017. He is currently pursuing the Ph.D. degree with the Robotics Laboratory, IIT Madras. His research interest includes robotics, design of haptic interfaces, control of teleoperation systems, such as adaptive robust control and neural network control, and development of mechatronic systems.

KARTHIK CHANDRASEKARAN received the Bachelor of Engineering degree in mechanical engineering from Anna University, India, in 2008, and the M.S. and Ph.D. degrees from IIT Madras, in 2020. From 2008 to 2011, he was with ELGI Equipment's Ltd., India, as a Research Engineer. He is currently an Assistant Professor with the School of Interdisciplinary Design and Innovation, Indian Institute of Information Technology, Design and Manufacturing, Kancheepuram. His research interests include teleoperated surgical robotics, medical device design, and application of compliant mechanisms to surgical tools.

SRIKAR ANNAMRAJU received the B.Tech. degree in instrumentation and control engineering from the National Institute of Technology Tiruchirappalli, India, in 2015, and the M.S. and Ph.D. degrees from IIT Madras, in 2020. He is currently an Assistant Professor with the Department of Electronics and Communication Engineering, Indian Institute of Information Technology, Design and Manufacturing, Kancheepuram. He works with modifying the teleoperation control architectures, passivity-based controllers, and impedance controllers. His research interests include control of teleoperation systems, particularly addressing issues of time delay.

ASOKAN THONDIYATH (Senior Member, IEEE) received the B.Tech. and M.Tech. degrees in mechanical engineering from Calicut University, India, in 1988 and 1991, respectively, and the Ph.D. degree from IIT Madras, India, in 2000. He completed a Postdoctoral Fellowship in medical device development with Stanford University. He was a Researcher with Nanyang Technological University, Singapore, researching on mechatronic systems and robotics for six years. He is currently a Professor with the Department of Engineering Design, IIT Madras.